Power Law Wave-Number Spectra of Scum on the Surface of a Flowing Fluid

Thomas M. Antonsen, Jr.,[1] Arthur Namenson,[2] Edward Ott,[1] and John C. Sommerer[3]
[1]*Department of Physics and of Electrical Engineering, University of Maryland, College Park, Maryland 20742*
[2]*Naval Research Laboratory, Washington, DC 20375*
[3]*M. S. Eisenhower Research Center, The Johns Hopkins Applied Physics Laboratory, Laurel, Maryland 20723-6099*
(Received 1 May 1995)

An initial cloud of particles floating on the surface of a flowing fluid will often tend to a fractal pattern. If the wave-number spectrum of the pattern has an observable power law dependence $k^{-\rho}$, then the exponent ρ is predicted to be $\rho = D_2 - 1$, where D_2 is the correlation dimension of the fractal attractor. Numerical, experimental, and theoretical results are shown to support this prediction, but it is also found that, when the observable range in k is limited, the predicted power law scaling can be obscured by fluctuations in the k spectrum. The expected behavior can, however, be restored by use of averaging.

PACS numbers: 05.45.+b, 47.20.–k, 68.10.Gw

Recent experimental [1] and theoretical [2] work has shown that particles floating on the surface of a flowing fluid can be attracted to a fractal distribution as time increases. The situation is analogous to a strange attractor of a dynamical system except that here the attractor exists in physical space (i.e., the fluid surface) rather than in an abstract phase space. Figure 1 shows an example illustrating the existence of a fixed point attractor (the point A) for floating particles on the surface of a fluid with a very simple steady flow. The point is that, with a slightly more complicated and time-dependent flow, attractors may still be present (as in Fig. 1), but they can be strange (i.e., fractal). Note that the particles on the surface can have an attractor even when the three-dimensional fluid flow is incompressible. We believe that this may be the mechanism responsible for the formation, commonly observed in nature, of convoluted spatial patterns of objects floating on bodies of water (e.g., algae, pollutants, etc.). (While throughout this paper our presentation is in the context of floaters, we emphasize that many of our considerations apply very generally to spatial patterns of multifractal measures [3].)

It is predicted [4] that the angle averaged wave-number power spectrum $F(k)$ of such a fractal pattern in the (two-dimensional) fluid surface is a power law, $F(k) \sim k^{-\rho}$, with exponent given by

$$\rho = D_2 - 1, \tag{1}$$

where D_2 is the correlation dimension [5] of the attractor. Here $F(k)$ is defined by

$$F(k) = (2\pi)^{-2} \int d^2\mathbf{k}' \delta(k - |\mathbf{k}'|)\overline{H}(\mathbf{k}'),$$

and $\overline{H}(\mathbf{k})$ is the Fourier transform of the two point correlation function $H(\mathbf{r}) = \langle \phi(\mathbf{x})\phi(\mathbf{x} + \mathbf{r})\rangle$, where the angle brackets indicate a spatial average over the domain $\mathcal{D}$ of the flow. In this paper, using numerical, experimental, and theoretical results, we investigate the applicability of (1). We find that, when the observable range in k is limited, the predicted power law scaling can be obscured by fluctuations, but that averaging can often restore the predicted scaling behavior, Eq. (1).

One way to derive (1) is to start with Parseval's theorem,

$$\int_{\mathcal{D}} \phi^2(\mathbf{x}) d^2\mathbf{x} = \int_0^\infty F(k)\, dk, \tag{2}$$

where $\phi(\mathbf{x})$ is the density of the floating particles, $\mathbf{x}$ is the spatial coordinate in the fluid surface, ϕ is normalized so that $\int \phi(\mathbf{x})\, d^2\mathbf{x} = 1$, and the $\mathbf{x}$ integration is over the area of interest. Imagine that there is some cutoff scale L_d for the finest variation of $\phi(\mathbf{x})$ (e.g., due to diffusion of the floating particles). Also assume a power law scaling range for $F(k)$, $L_d^{-1} \gg k \gg L_0^{-1}$, where L_0 is the overall scale size of the flow. We estimate $\int \phi^2\, d^2\mathbf{x} \sim \sum_i \phi_i^2 L_d^2$, where the fluid surface has been divided into a square grid of boxes of size L_d, and ϕ_i is the value of $\phi(\mathbf{x})$ in the middle of the ith box. We now associate a measure μ_i with each box, $\mu_i \equiv \int_{\text{box}\,i} \phi\, d^2\mathbf{x} \sim \phi_i L_d^2$. Thus $\int \phi^2\, d^2\mathbf{x} \sim L_d^{-2} \sum \mu_i^2$. From the definition of the correlation dimension, $\sum \mu_i^2 \sim L_d^{D_2}$, which then yields

$$\int \phi^2\, d^2\mathbf{x} \sim L_d^{-(2-D_2)}. \tag{3}$$

Assuming that $F(k) \sim k^{-\rho}$ with a large k cutoff at $k \sim L_d^{-1}$, the right hand side of (2) is of order $L_d^{-(1-\rho)}$. Combining this with (3) then yields (1) for the exponent ρ [6].

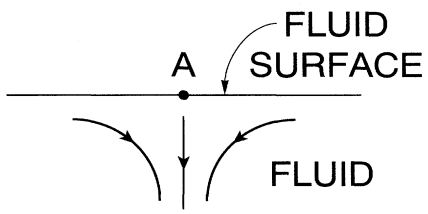

FIG. 1. The floating particles move toward point A.

 0031-9007/95/75(19)/3438(4)$06.00

We now consider a numerical test of (1). To do this we utilize a random version [2] of the Zaslavsky map [7], $x_{n+1} = [x_n + y_n(1 - e^{-\alpha})/\alpha] \mathrm{mod} 2\pi, y_{n+1} = \kappa \sin(x_{n+1} + \theta_n) + e^{-\alpha} y_n$, where θ_n is chosen randomly in $[0, 2\pi]$ at each iterate (for $\theta_n = 0$ we recover the map in [7]). As discussed in [2], this map models the motion of particles floating on the surface of a fluid in which there is a horizontal shear flow, vertical downwelling ($\alpha > 0$), and temporally irregular horizontal vortical motion [the term $\kappa \sin(x_{n+1} + \theta_n)$]. The Jacobian determinant of our map is independent of x and y and is equal to $e^{-\alpha} < 1$. Thus, areas are uniformly contracted by the map. This contraction property of the floating particles is due to the vertical downwelling flow component (cf. Fig. 1). In what follows we take $\alpha = 0.09$ and $\kappa = 0.5$.

We generate "snapshot attractors" [1,2,4,8] by randomly sprinkling 10^6 initial conditions uniformly in $0 \leq x \leq 2\pi, -2 \leq y \leq 2$, then iterating each such initial condition using the same random realization of the sequence of phase angles $\{\theta_n\}$ for each orbit, and recording the pattern after $\sim 10^2$ iterations. Figure 2 shows an example of a snapshot attractor obtained in this way.

Using many different random realizations of the sequence $\{\theta_n\}$, different snapshots were obtained. For each snapshot we performed a box-counting determination of the correlation dimension using the standard procedure of log-log plotting the correlation versus box size and estimating D_2 as the slope of the best fit straight line. For all snapshots very nice straight line behavior was observed, all with nearly the same slope. We estimate from these data that $D_2 = 1.39 \pm 0.01$.

Wave-number spectra were obtained for each of 20 snapshots. Figure 3(a) shows a log-log plot of one of these spectra. Power law dependence corresponds to a straight line on this plot. While Fig. 3(a) is roughly consistent with a linear decrease with large fluctuations superposed, the result is not very convincing. On the other hand, a much more convincing linear (i.e., power law) decrease is obtained by averaging the 20 spectra. This averaged spectrum $\langle F \rangle$ is shown in Fig. 3(b). Furthermore, the slope of the best fit straight line to the data in Fig. 3(b) yields $\overline{\rho} = 0.382 \pm 0.004$. This compares very well with the predicted value 0.39 ± 0.01 obtained from box counting and Eq. (1).

We interpret the evident power law obtained by averaging [Fig. 3(b)] as resulting from fluctuations in the k spectrum that vary randomly from snapshot to snapshot. The result of Fig. 3(b) can be understood if the fluctuation component tends to cancel upon averaging, thus leaving the pure power law component.

As a further test of (1), we have calculated the information dimension D_1 by box counting. Inserting the result for D_1 in place of D_2 in (1), we obtain $\rho = 0.50 \pm 0.01$. This result is clearly at odds with the result $\rho = 0.382 \pm 0.004$ obtained from Fig. 3(b), thus supporting the contention that the correlation dimension D_2 is the proper dimension to use.

We have also tested the applicability of (1) using data from the physical experiment on particles floating on a fluid surface described in Ref. [1]. In that experiment, a large number of tiny fluorescent spheres were distributed on the surface of a fluid initially at rest in a chamber with an annular barrier coming almost to the free surface. Fluid was pumped, for a fixed interval, up from the bottom of the outer portion of the chamber; it flowed over the barrier and out a central drain. The fluid was then allowed to come

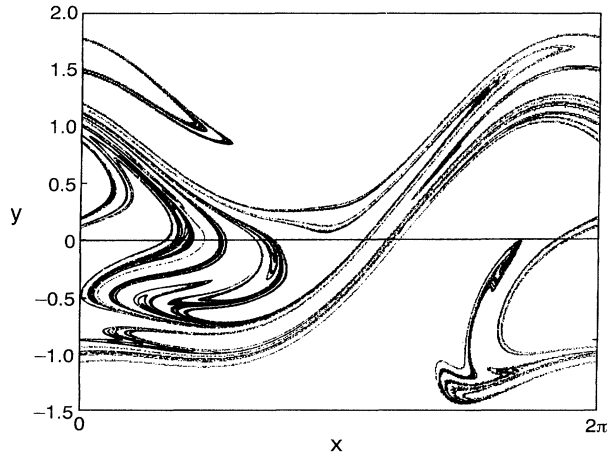

FIG. 2. Pattern formed by 10^6 randomly placed initial conditions after 10^2 iterates of the random Zaslavsky map with $\alpha = 0.09$ and $\kappa = 0.5$.

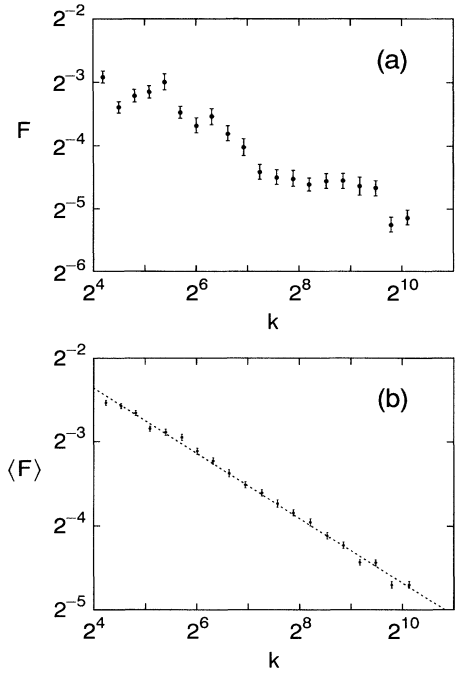

FIG. 3. (a) $F(k)$ versus k for one of the snapshots. (b) Plot of the average spectrum (denoted $\langle F \rangle$) versus k.

to rest, and the particle distribution was imaged via fluorescence. This sequence was repeated. Thus, there is a close correspondence between the motion of the floating particles in the physical experiment and a mapping in a phase plane. In the absence of fluid instabilities, the particles would be expected to clump together over the central drain. However, fluid instabilities created a recirculation cell structure, which varied in orientation at each pumping interval. These instabilities produced local stretching, in addition to the global dissipation resulting from the annular chamber. The randomly changing predominant orientation of the recirculation makes the most appropriate low-dimensional model of the surface flow a random mapping (strong evidence for the appropriateness of this model is presented in Ref. [1]).

After a brief transient, the particles accumulated on an approximately fractal attractor (with excellent scaling over more than a factor of 100 in box size) that changed shape from forcing period to forcing period. Agreement between the spatial pattern's measured information dimension (which remained nearly constant) and the Lyapunov dimension induced by the surface dynamics showed that the system was well modeled as a random mapping, similar to that used in our numerical example.

Angle-averaged wave-number spectra were obtained from a series of snapshots in the experiment; the snapshots were separated by at least five forcing periods. In this respect, the results from the physical experiment differ from those discussed above, where each snapshot resulted from a completely different realization of the random process. Assuming the dynamical process is stationary, time averaging and ensemble averaging should be equivalent. Note that, in physical experiments, time averaging will often be more feasible than ensemble averaging.

Figure 4 shows the observed wave-number spectrum for a particular flow condition. The spectral rolloff predicted from the correlation dimension ($D_2 = 1.28 \pm 0.04$) of the particle distribution is consistent with the averaged measured spectrum. Individual spectra show poorer agreement; as with the numerical results, averaging seems essential to observe the predicted power law dependence in the wave-number spectrum. The information dimension ($D_1 = 1.61 \pm 0.04$) of the observed particle distributions would, as in the numerical case above, predict the wrong scaling for the wave-number spectrum. Finally, it should be noted that similar agreement was observed for a different flow condition in the experiment. A fuller treatment of these experimental results is given in Ref. [8].

To further explore the issue of averaging, we now consider a simple example which is amenable to analytical treatment. In particular, we examine a random version of the generalized baker's map,

$$x_{n+1} = \begin{cases} \lambda x_n + a_n, & \text{if } y_n < \frac{1}{2}, \quad (4a) \\ \lambda x_n + \frac{1}{2} + b_n, & \text{if } y_n < \frac{1}{2}, \quad (4b) \end{cases}$$

$$y_{n+1} = 2y_n \bmod 1, \quad (4c)$$

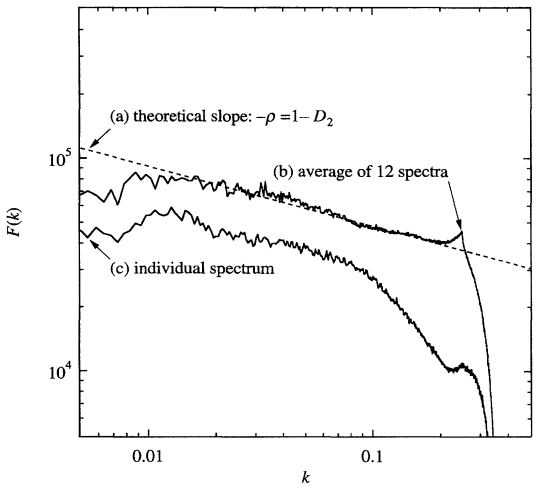

FIG. 4. Plot for the experiment [1] of (a) spectral rolloff predicted by Eq. (1); (b) average of 12 wave-number spectra; (c) the wave-number spectrum of an individual snapshot (displaced downward for clarity).

where $0 < \lambda < \frac{1}{2}$, and a_n and b_n are randomly chosen on each iterate n and are contained to lie between 0 and $\frac{1}{2} - \lambda$. Say that at some time far in the past, $n = -n_-$ where $n_- \gg 1$, a smooth density of orbit points $\phi_{-n_-}(x)$ was initialized. [Here, since the natural measure generated by (4) is uniform in $0 < y < 1$, we consider the measure (density) projected onto the x axis; thus we are considering an effectively one-dimensional problem.] At any positive time n, as $n_- \to +\infty$, the resulting density $\phi_n(x)$ approaches a fractal measure whose dimension D_2 is given by [4] $D_2 = \ln 2/\ln(1/\lambda)$. [Note that [4] the one-dimensional version of (1) is $\rho = D_2$.]

Now we consider the Fourier transform $f_n(k)$ of the density $\phi_n(x)$. Making use of (3), we can express the density at time $n + 1$ in terms of the density at time n,

$$\phi_{n+1}(x) = (2\lambda)^{-1}\left\{\phi_n[(x - a_n)/\lambda] + \phi_n\left[\left(x - b_n - \frac{1}{2}\right) \Big/ \lambda\right]\right\}.$$

Inserting this in the definition of the Fourier transform, we have $f_{n+1}(k) = \frac{1}{2}\{\exp(-ika_n) + \exp[-ik \times (b_n + \frac{1}{2})]\} f_n(\lambda k)$. Writing $F_n = |f_n|^2$, this becomes $F_{n+1}(k) = \cos^2(kc_n)F_n(\lambda k)$, where $c_n = \frac{1}{2}(b_n - a_n + \frac{1}{2})$. Successive application of this result leads to an explicit expression for $F_n(k)$ in the limit $n_- \to \infty$,

$$F_n(k) = \prod_{j=1}^{\infty} \cos^2(kc_{n-j}\lambda^{j-1}), \quad (5)$$

where we have made use of $F_n(0) = 1$.

We now average the relation $F_{n+1}(k) = \cos^2(kc_n)F_n(\lambda k)$ over the random variables c_m for $m = n, n-1, \ldots, -n_-$. Since the c_m are independent,

and $F_n(\lambda k)$ depends on c_m for $m \leq n-1$, we have that $\cos^2(kc_n)$ and $F_n(\lambda k)$ are independent. Thus $\langle F_{n+1}(k)\rangle = \langle \cos^2(kc_n)\rangle \langle F_n(\lambda k)\rangle$. For sufficiently large k, the quantity kc_n ranges over many intervals of 2π as c_n ranges over its possible values; thus $\langle \cos^2(kc_n)\rangle \cong \frac{1}{2}$ for large k. For $n_- \to \infty, \langle F_n(k)\rangle$ becomes independent of n. Hence for large k and $n_- \to \infty$,

$$\langle F(k)\rangle = \tfrac{1}{2}\langle F(\lambda k)\rangle . \tag{6}$$

Thus, when k is increased by a factor of λ^{-1}, the quantity $\langle F(k)\rangle$ decreases by a factor of $\frac{1}{2}$. In other words, $\langle F(k)\rangle$ conforms to a power law with the expected exponent, $\ln 2/\ln\lambda^{-1}$. Note, however that (6) also allows a periodic oscillation of $\langle F\rangle$ as a function of $\log k$ superposed on the general power law, and this oscillation, if present, would have a period $\log\lambda^{-1}$.

On the other hand, a log-log plot of the unaveraged quantity $F_n(k)$ [given by (5)] is extremely irregular due to the fact that $\log F_n(k) = -\infty$ at all the zeros of the individual cosines (i.e., at the values of k where $kc_{n-j}\lambda^{j-1}$ is an odd integer multiple of $\pi/2$). This is illustrated in Fig. 5 where we plot numerically generated spectra using Eq. (5). Shown in the plot is a single realization where a_n and b_n are selected randomly (we take a_n and b_n to be uniformly distributed in the interval $[0, (\frac{1}{2} - \lambda)]$). Also shown is the plot of the average spectrum generated by replacing $\cos^2(kc_{n-j}\lambda^{j-1})$ in Eq. (5) by its analytical average. As can be seen, the average spectrum produces a clear power law satisfying $\rho = \ln 2/\ln\lambda^{-1}$, with a superposed periodic oscillation with period in $\log k$ of $\log\lambda^{-1}$. In contrast, the individual realization shows large fluctuations. We have also examined the effect of randomly varying the parameter λ as well as the parameters a and b from iterate to iterate. In that case we find that, for large k, the oscillations are eliminated, and the averaged spectrum approaches a straight line on a log-log plot.

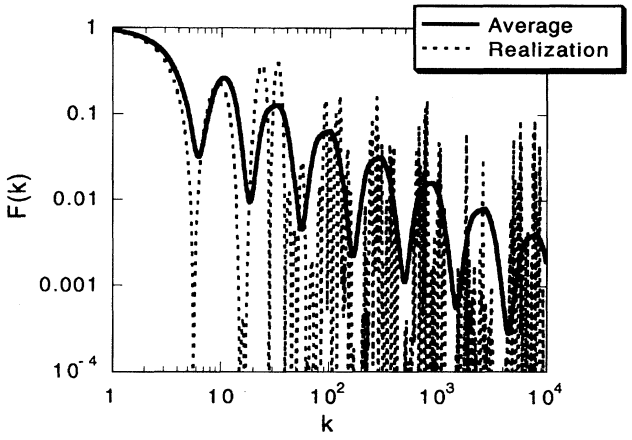

FIG. 5. Plot for the random baker's map of $F(k)$ for a single realization and of $\langle F\rangle$.

The work of T. M. A. and E. O. was partially supported by the Office of Naval Research. The work of J. C. S. was supported by the Space and Naval Warfare Systems Command. We thank A. S. Pikovsky for pointing out Ref. [6].

[1] J. C. Sommerer and E. Ott, Science **259**, 335 (1993); J. C. Sommerer, Physica (Amsterdam) **76D**, 85 (1994).

[2] L. Yu, E. Ott, and Q. Chen, Phys. Rev. Lett. **65**, 2935 (1990); Physica (Amsterdam) **53D**, 102 (1991).

[3] For example, two other potentially relevant physical situations are the fractal patterns of magnetic fields on the surface of the sun [e.g., L. Tao *et al.*, Astrophys. J. **443**, 434 (1995); A. C. Balke *et al.*, Sol. Phys. **143**, 215 (1993)], and of particles convected through the *volume* of a fluid subject to Stokes drag, buoyancy, and particle inertia [e.g., A. Crisanti *et al.*, Phys. Fluids A **4**, 1805 (1992); O. A. Druzhnin *et al.*, Chaos **3**, 359 (1993); L. P. Wang *et al.*, Phys. Fluids A **4**, 1789 (1992); L. Yu *et al.*, in *Nonlinear Structures in Physical Systems,* edited by L. Lam and H. C. Morris (Springer, New York, 1990)].

[4] A. Namenson, T. M. Antonsen Jr., and E. Ott (to be published).

[5] The correlation dimension was introduced by P. Grassberger and I. Procaccia, Phys. Rev. Lett. **50**, 346 (1983). The correlation dimension of a fractal measure in a two-dimensional space is defined as follows. First place a uniform grid of squares of edge length ϵ on the space. Then obtain $\mu_j(\epsilon)$, the measure in square j. Then calculate the "correlation" $I_2(\epsilon) = \sum \mu_j^2(\epsilon)$. The correlation dimension is then $D_2 = \lim_{\epsilon\to 0} \log[I_2(\epsilon)]/\log\epsilon$. The information dimension D_1 is defined similarly but with the information $I_1(\epsilon) = \sum \mu_j(\epsilon)\log\mu_j(\epsilon)$, replacing $\log[I_2(\epsilon)]$ in the limit.

[6] A different but analogous situation arises in the case of a frequency spectrum with fractal support (i.e., a singular continuous spectrum) for which the time correlation function decays as a power law in time with an exponent give by D_2. [For example, see R. Ketzmerick, G. Petschel, and T. Geisel, Phys. Rev. Lett. **69**, 695 (1992); A. S. Pikovsky, M. A. Zaks, U. Feudel, and J. Kurths, Phys. Rev. E **52**, 285 (1995), and references therein.]

[7] G. M. Zaslavsky, Phys. Lett. **69A**, 145 (1978).

[8] J. C. Sommerer (to be published).